DOI: 10.1002/ejic.201100857

Important Steric Effects Resulting from the Additional Substituent at Boron within Scorpionate Complexes Containing κ^3-*NNH* Coordination Modes

Nikolaos Tsoureas,[a] Rebecca F. Hope,[a] Mairi F. Haddow,[a] and Gareth R. Owen*[a][‡]

Keywords: N ligands / Ruthenium / Steric hindrance / Boron / Hydrides

The complexes [Ru(**Tai**)H(PPh_3)$_2$] (**4**) [**Tai** = HB(7-azaindolyl)$_3$] and [Ru(^{Ar}**Bai**)H(PPh_3)$_2$] [^{Ar}**Bai** = Ar(H)B(7-azaindolyl)$_2$; Ar = phenyl (**5**), mesityl (**6**) and 2-naphthyl (**7**)] have been prepared and fully characterised. Structural characterisation of complexes **4**, **5** and **7** confirmed the expected κ^3-*NNH* coordination mode of the azaindolyl-based ligands. In all complexes, the borohydride unit is located *trans* to the hydrido ligand, and the two triphenylphosphane ligands occupy sites *trans* to the two nitrogen donors. The strong Ru···H–B interaction means that the third substituent at the boron atom is held in close proximity to the ruthenium centre. In the case of complex **7**, rotation of the naphthyl group about the boron centre is hindered by the triphenylphosphane substituents.

Introduction

Over the course of the past few years we have carried out a wide range of investigations focused on the coordination chemistry and subsequent reactivity of **Tai** [tris(azaindolyl)-hydridoborate] (Figure 1) originally developed by Wang and co-workers in 2005.[1] This ligand is one of a new generation of flexible scorpionates[2] that have displayed new and exciting reaction pathways as well as activation of the boron–hydrogen bond (Figure 2).[3] This reactivity provided the first synthetic route to the elusive transition-metal–borane complexes.[3–7] Additional synthetic routes have subsequently been developed;[8,9] this field has recently been reviewed.[10] For some time now we have been interested in potential applications resulting from the reversible activation of the metal–boron bond.[4,11] In one recent development we have shown that it is possible to "recharge" the borane group with additional hydrogen by a 1,2-addition of H_2 across the metal–borane bond.[4f]

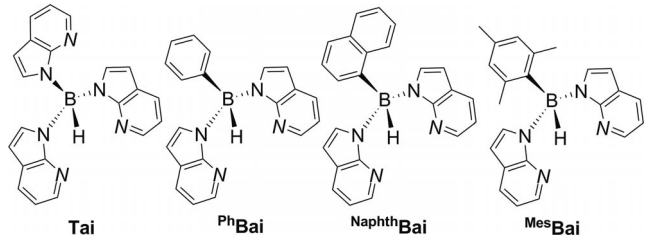

Figure 1. Four flexible scorpionate ligands based on 7-azaindole.

To date only a handful of ligand systems have been reported in which the N–L group, as shown in Figure 2, contains a three-atom bridge. Although κ^3-*LLH* coordination motifs are commonly observed for the archetypal Trofimenko-type scorpionate ligands,[12] they do not exhibit the reactivity shown in Figure 2, as this would lead to four-membered rings. The various three-atom bridging groups that have been developed and investigated are shown in Figure 3.

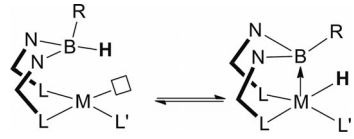

Figure 2. Hydride migration between boron and transition-metal centres (N–L = three-atom bridge in which L and L′ are donor groups).

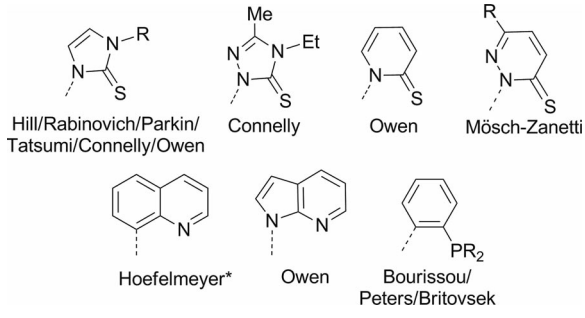

Figure 3. Current three-atom bridging groups that have been utilised to support transition-metal–borane complexes (* additional bonding interactions are involved in the reported examples featuring this group).

Our recent investigations have focused on obtaining a better understanding of the factors that govern hydride migration. We have studied a range of ligand systems and prepared a number of derivative ligands[4a,11c,11d] based on the

[a] The School of Chemistry, University of Bristol, Cantock's Close, Bristol, BS8 1TS, UK
E-mail: gareth.owen@bristol.ac.uk
[‡] Royal Society Dorothy Hodgkin Research Fellow

parent ligand **Tai** (Figure 1).[1] Replacing one of the azaindole rings with an aryl group appears to inhibit hydride migration in the resulting compounds as it has not been observed in any of the ^{Ar}**Bai** (Ar = phenyl, 2-naphthyl, mesityl) derivatives. A key difference between **Tai** and ^{Ar}**Bai** is the replacement of an electronegative nitrogen substituent at the boron atom by a carbon-based substituent. To explore this further we expanded the range of compounds to gain further insight into potential B–H activation. Herein, we report the synthesis and characterisation of a number of ruthenium complexes containing the four 7-azaindole-based ligands **Tai**, ^{Ph}**Bai**, ^{Mes}**Bai** and ^{Naphth}**Bai**. Three of these complexes have been structurally characterised and compared with previously reported examples to determine how the B–H···Ru interaction varies between the range of complexes. In the case of ^{Naphth}**Bai**, hindered rotation of the naphthyl group, which is held in close proximity to the metal centre due to a strong B–H···Ru interaction, is observed resulting from a steric clash with the triphenylphosphane co-ligands.

Results and Discussion

Synthesis and Characterisation of 4–7

We recently reported the benzylidene–ruthenium complexes [RuCl{κ^3-*NNH*-R(H)B(azaindolyl)$_2$}{=C(H)Ph}(PCy$_3$)] [R = azaindolyl (**1**), phenyl (**2**)] and [RuCl{κ^3-*NNH*-HB(azaindolyl)$_3$}{PCy$_2$(C$_6$H$_9$)}(PCy$_3$)] (**3**; Figure 4).[11c] Within these complexes very strong interactions were observed between the ruthenium centre and the borohydride units, as confirmed by their spectroscopic and structural characterisation (Table 1). A comparison of these compounds and other literature examples revealed that such interactions are particularly strong in those cases in which the borohydride unit is located *trans* to a halide or similar π-donor ligand.[11c] This is in contrast to examples in which the borohydride unit is located *trans* to a strong σ-donor such as hydride or alkyl groups. In these cases the interaction appears to be weaker. We suggested that a π-donation effect of the halide pushes electron density into the antibonding orbital (σ*) of the B–H bond. To explore this concept further we prepared a range of complexes analogous to **1**–**3** in which the borohydride unit would be positioned *trans* to a hydrido ligand to allow a direct comparison.

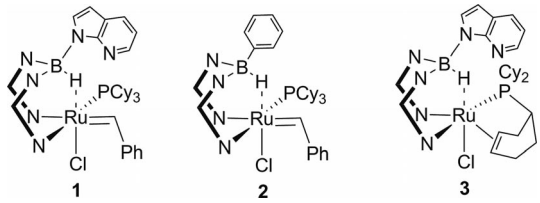

Figure 4. Previously reported complexes **1**–**3** (N–N = azaindolyl).

The complexes [Ru{κ^3-*NNH*-HB(azaindolyl)$_3$}H(PPh$_3$)$_2$] (**4**) and [Ru{κ^3-*NNH*-Ar(H)B(azaindolyl)$_2$}H(PPh$_3$)$_2$] [Ar = phenyl (**5**), mesityl (**6**), naphthyl (**7**)] were prepared by the reaction of stoichiometric quantities of K[**Tai**] and Li[^{Ar}**Bai**] (Ar = phenyl, mesityl, naphthyl), respectively, with [RuCl(H)(PPh$_3$)$_3$][13] in THF (Scheme 1). The resulting mixtures were heated at reflux until all of the starting materials had been consumed (as determined by ^{31}P{^{1}H} and ^{11}B{^{1}H} NMR spectroscopy). The ^{31}P{^{1}H} NMR spectra of the mixtures indicated the formation of the target products together with a signal corresponding to free triphenylphosphane. The uncoordinated triphenylphosphane proved difficult to remove from the products during their isolation. To achieve this separation, the free phosphane was oxidised in situ by the addition of H_2O_2 in the case of **4** or treated with an excess of MeI (to form [Ph$_3$PMe]I) in the cases of **5**, **6** and **7**. Complexes **4**–**7** were subsequently separated from Ph$_3$P(O) or [Ph$_3$PMe]I by passing a DCM solution of these mixtures through a plug of silica gel or neutral alumina.

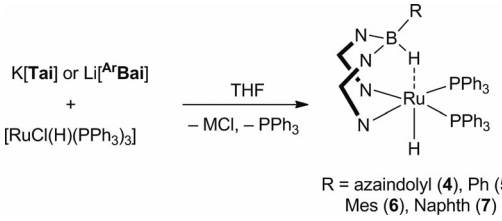

Scheme 1. Synthesis of complexes **4**–**7**.

The four complexes **4**–**7** were fully characterised by spectroscopic and analytical methods. Table 1 provides a summary of selected characterisation data along with those of the analogous complexes **1**–**3**. The ^{11}B{^{1}H} NMR spectrum of **4** reveals a single peak at δ = –0.4 ppm (h.h.w. = 35 Hz).

Table 1. NMR and IR spectroscopic data for ruthenium complexes containing 7-azaindole-based ligands.

Complex	δ [ppm]			$^1J_{B-H}$ [Hz]	$\tilde{\nu}$ [cm^{-1}]	
	^{1}H (Ru–*H*)	^{1}H (B–*H*···Ru)	^{11}B		B–H···Ru[a]	Ru–H[a]
[Ru(**Tai**)Cl{=CHPh}(PCy$_3$)] (**1**)[b]	–	–14.30	–0.8[b]	49	1929	–
[Ru{(^{Ph}**Bai**)Cl{=CHPh}(PCy$_3$)] (**2**)[b]	–	–14.20	–1.1[b]	u.r.[c]	1922	–
[Ru{**Tai**}Cl{PCy$_2$(η^2-C$_6$H$_9$)}] (**3**)[d]	–	–9.01	–0.3[d]	54	[e]	–
[Ru(**Tai**)H(PPh$_3$)$_2$] (**4**)[b]	–13.44	–2.44	–0.4	76	2076	1899
[Ru(^{Ph}**Bai**)H(PPh$_3$)$_2$] (**5**)[f]	–13.63	–2.93	–2.2	u.r.[c]	2068	1897
[Ru(^{Mes}**Bai**)H(PPh$_3$)$_2$] (**6**)	–13.93[d]	–2.03[d]	–0.8[b]	u.r.[c]	2078	1895
[Ru(^{Naphth}**Bai**)H(PPh$_3$)$_2$] (**7**)[b]	–13.95	–2.15	–1.8	u.r.[c]	2080	1899

[a] Powder film. [b] NMR experiment carried out in [D$_8$]toluene. [c] The B–H coupling constant was unresolved due to the broad nature of the signal. [d] NMR experiment carried out in [D$_6$]benzene. [e] Not determined. [f] NMR experiment carried out in [D$_2$]DCM.

The $^1J_{BH}$ coupling constants were determined by a boron-coupled (^{11}B) NMR experiment and can provide further information regarding the strength of the Ru···H–B interaction. In the ^{11}B NMR experiment of **4**, the signal appears as a doublet ($^1J_{BH}$ = 76 Hz) as a result of coupling to the adjacent hydrogen atom. The coupling constant observed for complex **4** is significantly larger than those of complexes **1** and **3** [cf. 49 (**1**) and 54 Hz (**3**)], which suggests a marked reduction in the B–H···Ru interaction in **4**. Thus, it appears that there is a weakening of the B–H bond as a result of a stronger Ru···H–B interaction in those cases in which the BH group is situated *trans* to a chlorido ligand. In the cases of the **^{Ar}Bai** complexes **5**–**7**, the ^{11}B{^{1}H} NMR spectra show broader signals at δ = –2.2 (h.h.w. = 134 Hz), –1.8 (h.h.w. = 260 Hz) and –1.8 (h.h.w. = 210 Hz) ppm, respectively. Unfortunately, this means that the one-bond B–H coupling constant could not be determined from the boron-coupled experiment. An increased linewidth of the boron signal is typical in complexes of this type and has previously been observed in other complexes containing aryl-substituted ligands.[4a,11c,11d] The ^{31}P{^{1}H} NMR spectra of **4**–**6** show singlet resonances between δ = 66.3 and 68.8 ppm. Conversely, the ^{31}P{^{1}H} NMR spectrum of **7** shows two broad resonances at δ = 66.1 and 70.3 ppm, which suggests fluxional behaviour within this complex at ambient temperatures. This is discussed in further detail below. The ^{1}H and ^{13}C{^{1}H} NMR spectroscopic data for **4** are consistent with the formation of [Ru{κ^3-*NNH*-HB(azaindolyl)$_3$}H(PPh$_3$)$_2$]. In contrast to previously reported rhodium and iridium (d^8) complexes,[4a,11a,11d] the NMR spectra of **4** reveal a static structure at room temperature, which indicates that the coordinated azaindolyl rings do not exchange with the uncoordinated ring at room temperature. The Ru*H* resonances for **4**–**7** appear as broadened triplet signals between δ = –13.44 and –13.95 ppm. These signals are more resolved in the corresponding ^{1}H{^{11}B} NMR spectra. In the case of **4**, the expected B*H* resonance appears as a 1:1:1:1 quartet at δ = –2.44 ppm ($^1J_{BH}$ = 75.6 Hz) in the standard ^{1}H NMR experiment, whereas the corresponding signals for **5**–**7** are unresolved. The resolution of the B*H* signal within the ^{1}H NMR spectrum of complex **4** is generally only observed within highly symmetrical compounds; however, a similar observation has previously been recorded in a related complex.[14] The most significant difference in the spectroscopic data for complexes **1**–**7** is the ^{1}H chemical shift of the B*H* unit. In complexes **4**–**7**, in which the Ru···H–B interaction is *trans* to the hydride, the B*H* signals are found between δ = –2.03 and –2.93 ppm. For complexes **1**–**3**, in which it is *trans* to a chlorido ligand, the signals are observed significantly shifted upfield [δ = –14.30 (**1**), –14.20 (**2**) and –9.01 (**3**) ppm]. The signals for complexes **1** and **2** are further upfield than those found for the terminal ruthenium hydride chemical shifts in **4**–**7** (Table 1). The formation of complexes **4**–**7** is also supported by the IR spectra, which show characteristic bands corresponding to both ruthenium–hydride and B–H···Ru stretching frequencies. In the solid state, bands ranging between 1895 and 1899 cm^{-1} are observed for the terminal hydride stretches, whereas bands between 2068 and 2080 cm^{-1} are observed for the B–H···Ru stretches (Table 1). These data all support the κ^3-*NNH* coordination mode of the four ligands in **4**–**7**. Finally, the molecular compositions of the complexes were confirmed by elemental analysis and mass spectrometry.

Variable-Temperature NMR Spectroscopy

Puerta and Valerga and co-workers recently reported a similar ruthenium hydride complex based on the sulfur-based ligand [HB(mt)$_3$]$^-$ (mt = *N*-methyl-2-mercaptoimidazolyl).[15] Within the complex [Ru{HB(mt)$_3$}H(PPh$_3$)$_2$] (**8**) a κ^3-*SSH* coordination mode is observed in the complex. Puerta and Valerga observed a solvent-dependent mixture of stereoisomers of **8** in which the terminal hydride is located either *cis* or *trans* to the B–H unit, the *trans* isomer being the dominant isomer in the solvents investigated. We found no evidence of this isomerisation within any of the complexes **4**–**7**. Although the ^{1}H NMR spectra of complexes **5** and **6** reveal one chemical environment for the azaindole units at ambient temperature, the corresponding spectrum for complex **7** shows particularly broad signals at these temperatures (Figure 5), which suggests fluxional behaviour. The aromatic region of this spectrum consists of six very broad signals integrating for 10 protons, corresponding to the two azaindole ring environments, and three broad resonances integrating for a total of 30 protons, corresponding to the two triphenylphosphane ligands. Seven comparatively sharp signals are also present in the same region, each integrating for one proton, corresponding to the naphthyl group.[16] The ^{13}C{^{1}H} NMR spectrum of **7** also shows broad signals at ambient temperatures, particularly those signals corresponding to the azaindole carbon atoms. As described above, the ^{31}P{^{1}H} NMR experiment shows two broad signals, which indicates the slow rotation of the naphthyl group. This rotation slowed further as the temperature was lowered, leading to two chemical environments for the two mutually *cis*-transposed triphenylphosphane ligands. Selected ^{31}P{^{1}H} NMR spectra recorded at

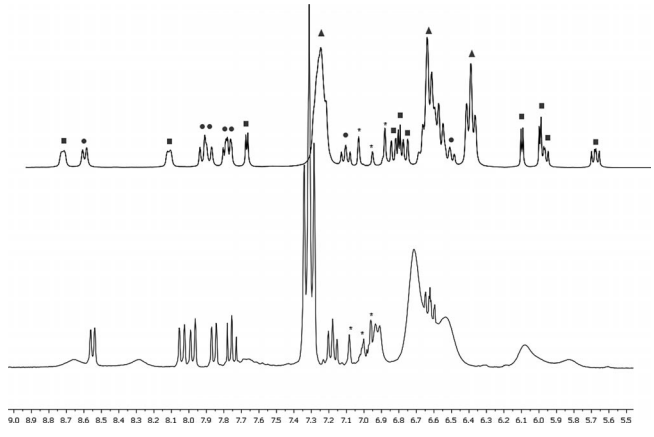

Figure 5. ^{1}H NMR spectra of [Ru{κ^3-*NNH*-BH(naphthyl)(azaindolyl)$_2$}H(PPh$_3$)$_2$] (**7**) recorded at –50 (top) and 22 °C (bottom). Signals assignment: squares = azaindolyl, dots = naphthyl, triangles = triphenylphosphane; * [D$_8$]toluene.

various temperatures are highlighted in Figure 6. As the temperature is lowered, the two signals resolve into two doublets, which confirms the distinct chemical environments of the phosphane ligands (Figure 7). At –50 °C the $^2J_{PP}$ coupling constant was found to be 32.6 Hz. In a similar way, the ^{1}H and ^{13}C{^{1}H} NMR spectra became more resolved as the temperature was lowered. At –50 °C, both spectra clearly show the two chemical environments of the azaindole ring in addition to the two chemical environments of the triphosphane ligands. The assignments of the ^{1}H and ^{13}C{^{1}H} NMR spectra at –50 °C are given in the Experimental Section below.

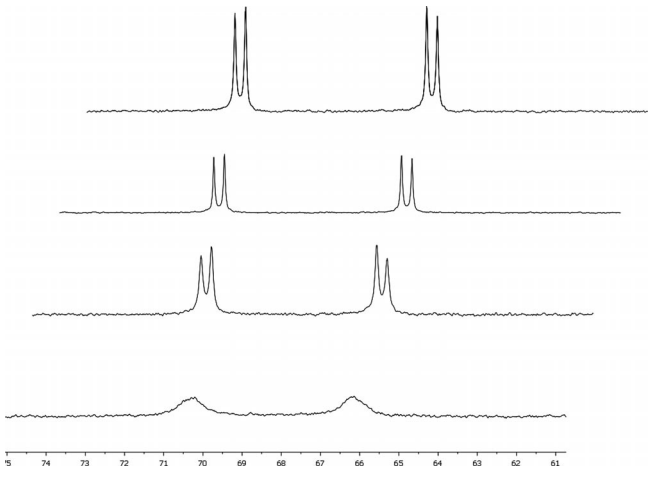

Figure 6. ^{31}P{^{1}H} NMR spectra of [Ru{κ^3-*NNH*-BH(naphthyl)-(azaindolyl)$_2$}H(PPh$_3$)$_2$] (**7**), showing the different chemical environments for the two PPh_3 ligands, recorded at –50, –20, 0 and 22 °C (top to bottom) in [D$_8$]toluene.

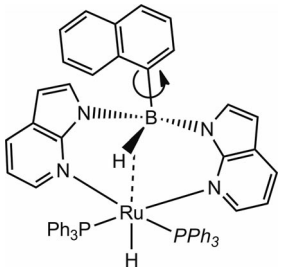

Figure 7. Rotation of the naphthyl group about the boron–carbon bond. The rotation is slow at room temperature and is slowed down further at lower temperatures (see main text for details).

X-ray Diffraction Studies

X-ray single-crystal diffraction studies were performed to further characterise our complexes and to establish the origin of the fluxional behaviour found in complex **7**. Single crystals of **4**, **5** and **7** were obtained by slow concentration of a saturated toluene solution of **4**, by leaving a pentane solution of **5** to stand at room temperature overnight and by leaving a saturated toluene solution of **7** to stand overnight. The molecular structures confirm the coordination of the azaindole-based ligands in each case (Figures 8, 9 and 10). Selected bond lengths and distances for **4**, **5** and **7** are highlighted in Table 2. Full details and crystallographic parameters are presented in Table 4. Although the isolated solid is spectroscopically and analytically pure, the single crystals of complex **5** contain some disordered chlorine atoms at the site of the hydrido ligand (see Crystallography in the Exp. Sect. for details), which indicates a chemical reaction involving the solvent (DCM) during the crystallisation of this compound. The transformation of transition-

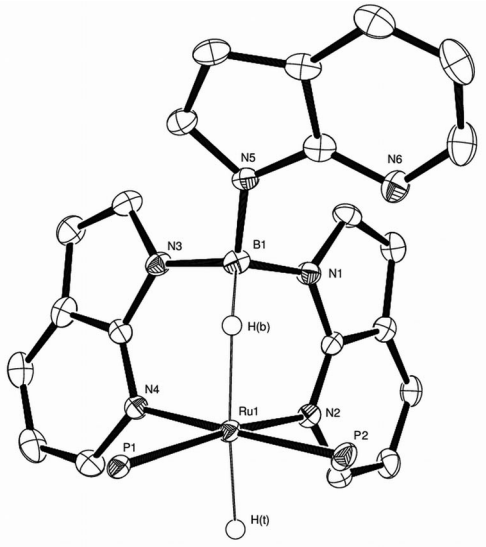

Figure 8. Molecular structure of [Ru{κ^3-*NNH*-HB(azaindolyl)$_3$}-H(PPh$_3$)$_2$] (**4**). The solvent molecule, phenyl groups from PPh_3 and hydrogen atoms, with the exception of H(t) and H(b), have been omitted for clarity (thermal ellipsoids drawn at the 50% probability level).

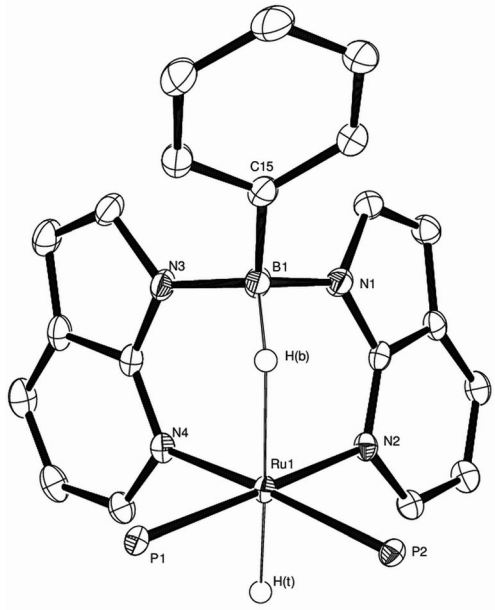

Figure 9. Molecular structure of [Ru{κ^3-*NNH*-Ph(H)B(azaindolyl)$_2$}H(PPh$_3$)$_2$] (**5**). The phenyl groups from PPh_3 and hydrogen atoms, with the exception of H(t) and H(b), have been omitted for clarity (thermal ellipsoids drawn at the 50% probability level).

metal hydride species to transition-metal chloride in chlorinated solvents has previously been observed.[17] Each complex adopts an octahedral geometry featuring the ligands **Tai**, ^{Ph}**Bai** or ^{Naphth}**Bai** with a κ^3-*NNH* coordination mode. This coordination motif consists of two azaindolyl moieties coordinating through the nitrogen atom of the pyridine heterocycles and a B–H interaction at an apical site on the ruthenium centre. The complexes are further coordinated by a hydrido ligand, which is located *trans* to the B–H group, and two triphenylphosphane ligands, which are located *cis* to each other and *cis* to the hydrido ligand. The angles involving the nitrogen and phosphane donor substituents, which are mutually *cis*-disposed, range between 84.45(4) and 97.332(13)° in the three structures. The smallest angles are found for N(2)–Ru(1)–N(4), whereas the largest angles are observed for P(1)–Ru(1)–P(2). This is expected for the bulky triphenylphosphane ligands.

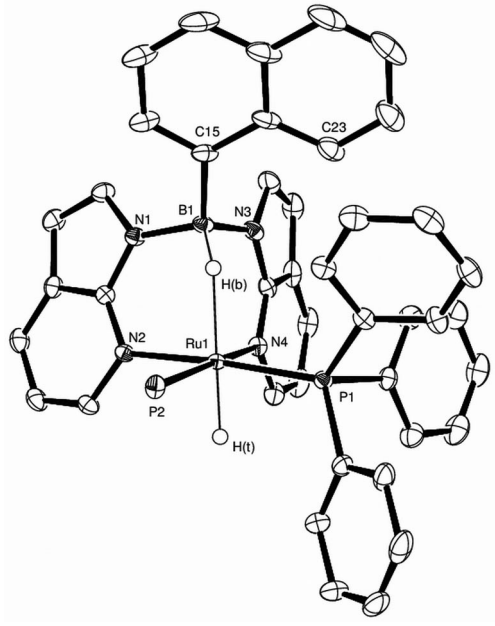

Figure 10. Molecular structure of [Ru{κ^3-*NNH*-Naphth(H)B(azaindolyl)$_2$}H(PPh$_3$)$_2$] (**7**). The solvent molecule, the three phenyl groups from one PPh$_3$ and hydrogen atoms, with the exception of H(t) and H(b), have been omitted for clarity (thermal ellipsoids drawn at the 50% probability level).

The two six-membered rings formed by the κ^3-*NNH* coordination motif of the azaindole-based ligands mean that the additional substituent at the boron atom is pulled towards the ruthenium centre. The extent to which this occurs is dictated by the strength of the interaction between the metal centre and the B–H group, which in turn is affected by the steric demands of the additional substituent. This can be seen when comparing the Ru···B distances in **8** and [Ru{H$_2$B(mt)$_2$}H(PPh$_3$)$_2$][14] (**9**). In these examples, the B–H unit is able to approach the metal centre more closely when the additional substituent is a hydrogen atom [cf. 2.931(8) Å for **8** and 2.774(3) Å for (**9**)]. This may have important consequences as to whether hydride migration to the metal centre is possible or not with various groups at the boron atom. The orientation of the substituent is also likely to be an important factor. In those cases, in which hydride migration is not observed, a κ^3-*NNH* coordination motif is always found. In the parent ligand **Tai**, which contains a third azaindolyl group, the heterocycle is found to be almost parallel to the B–H···metal direction in the group nine complexes [Rh(**Tai**)(cod)] (**10**), [Ir(**Tai**)(cod)] (**11**) and [Rh(**Tai**)(nbd)] (**12**) (cod = 1,5-cyclooctadiene; nbd = 2,5-norbornadiene). The torsion angles (defined by M···B–N–C) for **10**–**12** were found to be 0.8(3), 1.0(5) and 0°, respectively. Within these complexes the diene co-ligands do not provide significant steric hindrance, and therefore the orientation of the heterocycle is not limited by steric

Table 2. Selected bond lengths and angles for complexes **4**, **5** and **7**.[a]

Bond lengths [Å] and angles [°]	**4**[b]	**5**[c]	**7**[d]
Ru(1)–N(2)	2.124(3)	2.1467(17)	2.1331(11)
Ru(1)–N(4)	2.136(3)	2.1482(17)	2.1384(12)
Ru(1)–P(1)	2.3046(10)	2.2874(7)	2.2864(4)
Ru(1)–P(2)	2.2764(11)	2.2981(6)	2.2948(4)
Ru(1)–H(t)	1.61(3)	1.56(3)[c]	1.524(18)
Ru(1)···H(b)B(1)	1.71(4)	1.85(2)	1.87(2)
B(1)–N(1)	1.532(6)	1.553(3)	1.5558(19)
B(1)–N(3)	1.542(5)	1.542(3)	1.543(2)
B(1)–N(5)/B(1)–C(15)	1.524(5)	1.611(3)	1.618(2)
N(1)–B(1)–N(5)/N(1)–B(1)–C(15)	109.6(3)	113.44(18)	111.25(12)
N(3)–B(1)–N(5)/N(3)–B(1)–C(15)	111.4(3)	112.16(17)	114.68(12)
N(4)–Ru(1)–N(2)	85.31(11)	85.80(6)	84.45(4)
P(2)–Ru(1)–N(2)	90.90(8)	89.82(5)	88.15(3)
P(1)–Ru(1)–N(4)	86.50(8)	89.18(5)	89.62(3)
P(1)–Ru(1)–P(2)	97.29(4)	94.92(2)	97.332(13)
Ru(1)–H(1)–B(1)	129(2)	132(2)	132(1)
$\sum$ of angles of non-hydrogen substituents at B	330.0	335.1	332.0
Position of Ar group at B[e]	73.0(5)	80.6(3)	79.2(2)

[a] Additional distances and angles for **4**, **5** and **7** can be found in Table 3. [b] This structure contains one molecule of toluene as solvent of crystallisation. [c] This complex was recrystallised from DCM and contains disordered chloride (in a Cl/H ratio of 15:85) in the position of H(t). [d] This structure contains one molecule of disordered toluene solvent of crystallisation. [e] Defined by the modulus of the smallest torsion angle M···B–C$_{ipso}$–C$_{ortho}$ (for ^{Ar}**Bai**) or M···B–N–C (for **Tai**).

Table 3. Distances [Å] and angles [°] for various azaindole-based ruthenium complexes containing a κ^3-*NNH* coordination mode.

Complex	Ru···B	N–B–N	Ref.
[Ru(**Tai**)Cl{=C(H)Ph}(PCy_3)] (**1**)	2.673(3)	114.7(13)	[11c]
[Ru(**^{Ph}Bai**)Cl{=C(H)Ph}(PCy_3)] (**2**)[a]	2.694(4)/2.675(4)	111.7(2)/112.0(2)	[11c]
[Ru(**Tai**)Cl{$PCy_2(\eta^2$-$C_6H_9)$}] (**3**)[a,b]	2.769(4)/2.766(4)	119.9(4)/112.3(4)	[11c]
[Ru(**Tai**)H($PPh_3)_2$] (**4**)	2.776(5)	109.0(3)	this work
[Ru(**^{Ph}Bai**)H($PPh_3)_2$] (**5**)	2.864(2)[c]	109.45(18)	this work
[Ru(**^{Naphth}Bai**)H($PPh_3)_2$] (**7**)	2.865(2)	106.03(11)	this work
[Ru(**Tai**)(Cp*)]	2.786(6)	112.1(5)	[1b]

[a] Two independent molecules within the same structure. [b] This structure contains one molecule of toluene solvent of crystallisation. [c] The B–H interaction with the metal centre is *trans* to disordered Ru–H and Ru–Cl within the structure.

bulk. In complex **4** and the previously reported complexes **1** and **3**, however, the corresponding torsion angles are different [cf. 73.0(5) (**4**), 73.5(3)° (**1**) and 73.1(5) and 77.0(5)° for the two independent molecules found in the unit cell in **3**]. In **^{Naphth}Bai** the azaindole ring has been replaced by a naphthyl group and was originally chosen to mimic the steric properties of the azaindole ring. For the complex [Rh(**^{Naphth}Bai**)(NBD)], the naphthyl group is orientated with torsion angles 69.1(5), 49.4(5) and 73(2)° for the three independent molecules in the unit cell. In **7**, the corresponding torsion angle is 79.2(2)°. Even though the solid-state structures reveal quite similar parameters for complexes **4** and **7** (Table 2), the solution-state NMR spectra are different (i.e., the rotation of the additional substituent is hindered in the case of naphthyl but not in the case of azaindolyl). This is intriguing, because the Ru(1)···B(1) distance is longer for **7** [2.839(2) Å] than it is for **4** [2.777(5) Å]. There is only a small difference in the steric space occupied between an azaindole and naphthalene ring, although the CH group (C23) of the naphthyl group points towards the bulky triphenylphosphane ligand (Figure 10). There are no clear indications from the two structures to confirm a significant difference between them. Finally, in the case of **5**, the phenyl group is orientated at an angle similar to that found in the group nine complexes [Rh(**^{Ph}Bai**)(cod)] [cf. 80.6(3) with 82.9(4)°] and [Ir(**^{Ph}Bai**)(cod)] [73.7(5)°] as well as in complex **2** [72.4(4)° and 73.4(3)°, two independent molecules in the unit cell].

As described above, the B–H···Ru interaction is dependent on the nature of the ligand *trans* to it. It is particularly strong when the B–H unit is located *trans* to a π donor. The characterisation of complexes **4**–**7**, in which the B–H unit is *trans* to a hydrido ligand, allows for a direct comparison with complexes **1**–**3** in which the unit is *trans* to a chlorido ligand. The pertinent distances and angles for these complexes are provided in Table 3 along with those of related literature compounds. The Ru···B distances are generally longer for the ruthenium hydride complexes. Furthermore, the corresponding N(3)–B(1)–N(1) angles are larger in those complexes in which the B–H group is *trans* to chloride rather than hydride [cf. 111.7(2)–114.7(13)° for complexes **1**–**3** to 106.03(11)–109.44(19)° for **4**, **5** and **7**].

Conclusions

A series of bis(triphenylphosphane)ruthenium hydride complexes containing the recently reported azaindolyl-based scorpionate ligands **Tai**, **^{Ph}Bai**, **^{Mes}Bai** and **^{Naphth}Bai** have been synthesised and characterised. The ligands coordinate to the ruthenium centres through a κ^3-*NNH* coordination mode. The interaction of the borohydride group with the metal centre is strong – however, not as strong as that found in ruthenium complexes containing a chlorido ligand *trans* to the BH unit. In addition, the strong κ^3-*NNH* coordination mode pulls the additional substituent at the boron atom towards the bulky triphenylphosphane ligands, as evidenced by the hindered rotation of the naphthyl group in **7**. Further investigations are underway to explore the steric effects of the additional substituent on the propensity of the borohydride function to undergo hydride migration.

Experimental Section

General: All manipulations were performed in a Braun glovebox with an O_2 and H_2O atmosphere of below 5 ppm or by using standard Schlenk techniques. [$RuCl(H)(PPh_3)_3$],[13] K[**Tai**],[1a] Li[**^{Ph}Bai**],[4a] Li[**^{Mes}Bai**][11d] and Li[**^{Naphth}Bai**][11d] were prepared according to literature procedures. The solvents (toluene, THF, DCM) were dried by using a Grubbs' alumina system. Dry *n*-pentane (< 0.05 ppm H_2O) was purchased from Fluka. Deuteriated toluene and benzene were degassed by three freeze-thaw cycles, dried by heating at reflux in the presence of Na or Na/benzophenone, respectively, for 12 h, vacuum distilled and stored over 4 Å molecular sieves. Deuteriated DCM was dried by heating at reflux in the presence of CaH_2 for 12 h. ^1H, $^{11}B\{^1H\}$, ^{11}B and $^{31}P\{^1H\}$ NMR spectra were recorded with a JEOL ECP300 spectrometer operating at 300 MHz (^1H). $^{13}C\{^1H\}$ NMR spectra and correlation experiments were recorded with a Varian VNMR S500 spectrometer operating at 500 MHz (^1H). The spectra are referenced internally to the residual protic solvent (^1H) or solvent signals (^{13}C). $^{11}B\{^1H\}$ and ^{11}B NMR spectra are referenced externally relative to $BF_3{\cdot}OEt_2$. $^{31}P\{^1H\}$ NMR spectra are referenced externally relative to 85% H_3PO_4 in D_2O. The atomic labelling for the azaindolyl (Aza), mesityl (Mes), phenyl (Ph) and naphthyl (Nap) groups in the ligands are shown in Figure 11. Mass spectra were recorded

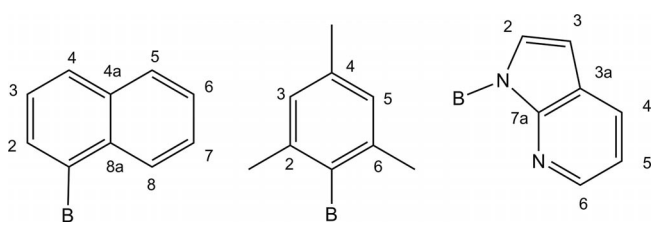

Figure 11. Numbering scheme for azaindolyl (Aza), mesityl (Mes), phenyl (Ph) and naphthyl (Nap) groups.

with a VG Analytic Quattro spectrometer in ESI$^+$ mode. Elemental analyses were performed at the microanalytical laboratory of the School of Chemistry at the University of Bristol. Infrared spectra were recorded with a Perkin–Elmer Spectrum 100 FTIR spectrometer (solid state, neat) in the range 4000–650 cm^{-1}.

[Ru{κ^3-*NNH*-B(H)(azaindolyl)$_3$}H(PPh$_3$)$_2$] (4): A Schlenk tube in a glovebox was charged with [RuHCl(PPh$_3$)$_3$] (153.8 mg, 0.166 mmol) and K[**Tai**] (67.5 mg, 0.166 mmol). THF (15 mL) was then added to give a purple suspension. The reaction mixture was heated at 70 °C for 20 min after which time a yellow solution was obtained. The ^{31}P{^{1}H}, ^{11}B{^{1}H} and ^{11}B NMR spectra revealed complete conversion of the starting materials. The mixture was cooled to 0 °C, and H_2O_2 (200 μL, 30 wt.-% solution) was added through a microsyringe. The mixture was warmed to room temperature after which all volatiles were removed under reduced pressure. The residue was then extracted with hexane (3 × 15 mL) and filtered through Celite™. The hexane extracts were contaminated with approximately 5% of triphenylphosphane oxide. All volatiles were removed, and the residue was redissolved in DCM (15 mL). The solution was passed through a plug of silica and washed with a further portion of DCM (15 mL). Again, all volatiles were removed under reduced pressure, and the residue was washed with *n*-pentane (5 mL) to provide **3** as a pale-yellow powder. Yield: 115 mg (70%). ^{1}H NMR (C_7D_8): δ = –13.44 [1 H, unresolved triplet (see ^{1}H{^{11}B} NMR data below), RuH], –2.44 (q, $^1J_{BH}$ = 75.6 Hz, 1 H, B-H), 5.87 (dd, $^3J_{HH}$ = 7.7, $^3J_{HH}$ = 5.5 Hz, 2 H, Aza 5-H), 6.13 (d, $^3J_{HH}$ = 3.3 Hz, 2 H, Aza 3-H), 6.66 (overlapping signals, virtual t, J_{PH} = 7.2 Hz, 12 H, *p*-PC$_6$H$_5$ and 1 H, Aza 3′-H), 6.78 (virtual t, J_{PH} = 7.0 Hz, *p*-PC$_6$H$_5$), 6.90 (dd, $^3J_{HH}$ = 7.7, $^4J_{HH}$ = 1.4 Hz, 2 H, Aza 4-H), 6.94 (dd, $^3J_{HH}$ = 7.8, $^3J_{HH}$ = 4.7 Hz, 1 H, Aza 5′-H), 7.44 (overlapping signals, m, 12 H, *o*-PC$_6$H$_5$ and 2 H, Aza 2-H), 7.81 (d, $^3J_{HH}$ = 3.5 Hz, 1 H, Aza 2′-H), 7.93 (dd, $^3J_{HH}$ = 7.8, $^4J_{HH}$ = 1.8 Hz, 1 H, Aza 4′-H), 8.16 (dd, $^3J_{HH}$ = 4.7, $^4J_{HH}$ = 1.8 Hz, 1 H, Aza 6′-H), 8.46 (d, $^3J_{HH}$ = 5.7 Hz, 2 H, Aza 6-H) ppm; the signals corresponding to Aza 2-H and 3′-H were located in an HMQC experiment. ^{1}H{^{11}B} NMR: δ = –13.44 (t, $^2J_{PH}$ = 26.6 Hz, 1 H), –2.44 (br. s, B-H) ppm. ^{13}C{^{1}H} NMR: δ = 101.6 (Aza C-3′), 102.3 (Aza C-3), 114.5 (Aza C-5), 115.5 (Aza C-5′), 123.2 (Aza C-7a) 123.9 (Aza C-7a′), 126.9 (virtual t, J_{PC} = 4.5 Hz, *m*-PC$_6$H$_5$),[18] 127.0 (Aza C-4), 127.3 (Aza C-4′), 128.1 (*p*-PC$_6$H$_5$, located in a DEPT-135 experiment), 131.3 (Aza C-2), 133.1 (Aza C-2′), 134.5 (virtual t, J_{PC} = 5.2 Hz, *o*-PC$_6$H$_5$),[18] 141.8 (Aza C-6′), 149.5 (Aza C-6), 153.2 (Aza C-3a′), 154.0 (Aza C-3a) ppm; *i*-PC$_6$H$_5$ signal not located. ^{31}P{^{1}H} NMR: δ = 68.8 (s, PPh$_3$) ppm. ^{11}B{^{1}H} NMR: δ = –0.44 (s, Δν$_{1/2}$ = 35 Hz) ppm. ^{11}B NMR: δ = –0.44 (d, $^1J_{BH}$ = 75.6 Hz) ppm. IR (neat): $\tilde{\nu}$ = 1899.1 (ν$_{RuH}$), 2075.8 (ν$_{BH}$) cm^{-1}. MS (ESI$^+$): *m*/*z* = 989.2 [M + H]$^+$, 727.16 [M + H – PPh$_3$]$^+$. $C_{57}H_{47}BN_6P_2Ru$ (989.87): calcd. C 69.16, H 4.79, N 8.49; found C 69.60, H 4.82, N 8.91.

General Procedure for the Preparation of [Ru{κ^3-*NNH*-B(H)(azaindolyl)$_2$(Aryl)}H(PPh$_3$)$_2$] (5–7): In a glovebox, a Schlenk tube was charged with [RuCl(H)(PPh$_3$)$_3$]·toluene (150 mg, 0.148 mmol) and [Li(THF)][^{Ar}**Bai**] (1 mol equiv.) and connected to a Schlenk line. Anhydrous THF (10 mL) was added at room temperature, and the purple suspension was heated at 65 °C for 1 h, upon which time a yellow solution was obtained and no starting material was detected by ^{31}P{^{1}H} and ^{11}B{^{1}H} NMR spectroscopy. The mixture was allowed to equilibrate at room temperature after which it was treated with MeI (3.22 mmol, 200 μL) and stirred at room temperature until no free PPh$_3$ could be detected in the ^{31}P{^{1}H} NMR spectrum (approximately 1.5 h). All volatiles were removed from the filtrate to give a yellow residue, which was extracted with DCM (3 × 10 mL) and filtered through a short plug of neutral alumina (5 × 5 cm) above a short plug of Celite, which were then washed with DCM until the washings were colourless. All volatiles were removed from the extracts, and the residue was washed with *n*-pentane (5 mL) and dried in vacuo to yield the products as yellow microcrystalline solids.

[Ru{κ^3-*NNH*-B(H)(azaindolyl)$_2$(phenyl)}H(PPh$_3$)$_2$] (5): Yield: 85 mg (61%). ^{1}H NMR (CD_2Cl_2): δ = –13.63 [unresolved t (see ^{1}H{^{11}B} data below), 1 H, Ru-H], –2.93 (br., 1 H, B-H), 6.15 (dd, $^3J_{HH}$ = 7.7, $^3J_{HH}$ = 5.1 Hz, 2 H, Aza 5-H), 6.20 (d, $^3J_{HH}$ = 3.3 Hz, 2 H, Aza 3-H), 6.80 (virtual t, J_{PH} = 7.0 Hz, 12 H, *p*-PC$_6$H$_5$), 6.98 (virtual t, 6 H, J_{PH} = 7.3 Hz, *p*-PC$_6$H$_5$), 7.08 (m, 12 H, *o*-PC$_6$H$_5$), 7.29 (dd, $^3J_{HH}$ = 7.7, $^4J_{HH}$ = 1.5 Hz, 2 H, Aza 4-H), 7.35 (d, $^3J_{HH}$ = 3.3 Hz, 2 H, Aza 2-H), 7.45 (m, 3 H, BC$_6$H$_5$), 7.73 (m, 2 H, BC$_6$H$_5$), 8.31 (d, $^3J_{HH}$ = 5.1 Hz, 2 H, Aza 6-H) ppm. ^{1}H{^{11}B} NMR: δ = –13.6 (t, $^2J_{PH}$ = 26.4 Hz, Ru-H), –2.93 (br. s, BH) ppm. ^{13}C{^{1}H} NMR: δ = 101.9 (Aza C-3), 114.9 (Aza C-5), 123.2 (Aza C-7a), 126.7 (*p*-BC$_6$H$_5$), 127.2 (two overlapping signals, virtual t,[18] J_{PC} = 4.4 Hz, *m*-PC$_6$H$_5$ and s, *m*-BC$_6$H$_5$), 127.9 (Aza C-4), 128.3 (*p*-PC$_6$H$_5$), 131.9 (Aza C-2), 134.33 (virtual t, J_{PC} = 5.2 Hz, *o*-PC$_6$H$_5$),[18] 135.6 (*o*-BC$_6$H$_5$), 137.7 [two overlapping signals, d, J_{PC} = 38.3 Hz, *i*-PC$_6$H$_5$ and br. s, *i*-BC$_6$H$_5$ (tentatively assigned)], 149.5 (Aza C-6), 155.5 (Aza C-3a) ppm. ^{31}P{^{1}H} NMR: δ = 68.8 ppm. ^{11}B{^{1}H} NMR: δ = –2.19 (s, Δν$_{1/2}$ = 133.9 Hz) ppm. ^{11}B NMR: δ = –2.19 (s, Δν$_{1/2}$ = 184.5 Hz) ppm. IR (neat): $\tilde{\nu}$ = 2068.4 (ν$_{BH}$), 1897.0 (ν$_{RuH}$) cm^{-1}. MS (ESI$^+$): *m*/*z* = 949.2 [M – H]$^+$, 973.2 [M + Na]$^+$, 990.2 [M – H + CH_3CN]$^+$. $C_{56}H_{47}BN_4P_2Ru$ (949.84): calcd. C 70.81, H 4.99, N 5.90; found C 70.64, H 5.20, N 6.02.

[Ru{κ^3-*NNH*-B(H)(azaindolyl)$_2$(mesityl)}H(PPh$_3$)$_2$] (6): Yield: 59 mg (40%). ^{1}H NMR (C_6D_6): δ = –13.93 (t, $^2J_{PH}$ = 28.3 Hz, 1 H, Ru-H), –2.03 (br., 1 H, BH), 2.10 (s, 6 H, 2,6-Me), 2.46 (s, 3 H, 4-Me), 5.94 (dd, $^3J_{HH}$ = 7.6, $^3J_{HH}$ = 5.4 Hz, 2 H, Aza 5-H), 6.13 (d, $^3J_{HH}$ = 3.5 Hz, 2 H, Aza 3-H), 6.70 (virtual t, J_{PH} = 7.4 Hz, 12 H, *m*-PC$_6$H$_5$),[18] 6.82, (virtual t, J_{PH} = 7.3 Hz, 6 H, *p*-PC$_6$H$_5$),[18] 7.01 (dd, $^3J_{HH}$ = 7.6, $^4J_{HH}$ = 1.2 Hz, 2 H, Aza 4-H), 7.10 [s, 2 H, C$_6H_2$(CH$_3$)$_3$], 7.29, (d, $^3J_{HH}$ = 3.5 Hz, 2 H, Aza 2-H), 7.36 (br., virtual t, J_{PH} = 8.2 Hz, 12 H, *o*-PC$_6$H$_5$),[18] 8.50 (d, $^3J_{HH}$ = 5.5 Hz, 2 H, Aza 6-H) ppm. ^{13}C{^{1}H} NMR (C_6D_6): δ = 21.6 (Mes 4-CH$_3$), 26.4 (Mes 2,6-CH$_3$), 102.5 (Aza C-3), 114.8 (Aza C-5), 123.8 (Aza C-7a), 127.1 (Aza C-4), 127.5 [virtual t, J_{PC} = 4.9 Hz, *m*-P(C$_6$H$_5$)$_3$],[18] 128.6 [s, *p*-P(C$_6$H$_5$)$_3$, overlapping with solvent peaks observed by a DEPT-135 experiment], 130.7 (Aza C-2), 133.2 (Aza C-6), 134.9 [virtual t, J_{PC} = 4.4 Hz *o*-P(C$_6$H$_5$)$_3$],[18] 135.7 (Mes C-2,6), 138.2 [m, *i*-P(C$_6$H$_5$)$_3$], 144.8 (Mes C-4), 150.1 (Mes C-3,5), 154.9 (Aza C-3a) ppm; carbon *ipso* to boron signal not observed. ^{31}P{^{1}H} NMR (C_7D_8): δ = 66.3 ppm. ^{11}B{^{1}H} NMR (C_7D_8): δ = –1.8 (s, Δν$_{1/2}$ = 260 Hz) ppm. ^{11}B NMR (C_7D_8): δ = –1.8 (s, Δν$_{1/2}$ = 295 Hz) ppm. MS (ESI$^+$): *m*/*z* = 992.3 [M]$^+$. IR (neat): $\tilde{\nu}$ = 2078 (ν$_{BH}$), 1895 (ν$_{RuH}$) cm^{-1}. $C_{59}H_{53}BN_4P_2Ru{\cdot}4/3CH_2Cl_2$ (1105.15): calcd. C 65.57, H 5.07, N 5.80; found C 65.90, H 4.99, N 5.79.

[Ru{κ^3-*NNH*-B(H)(azaindolyl)$_2$(2-naphthyl)}H(PPh$_3$)$_2$] (7): Yield 77 mg, (48%). NMR spectra recorded at –50 °C. ^{1}H NMR (C_7D_8): δ = –13.95 (t, $^2J_{PH}$ = 26.4 Hz, 1 H, Ru-H), –2.15 (br., 1 H, BH, Δν$_{1/2}$ = 67 Hz), 5.81 (dd, $^3J_{HH}$ = 7.9, $^3J_{HH}$ = 5.5 Hz, 1 H, Aza 5-H), 6.10 (overlapping with adjacent signal, dd, $^3J_{HH}$ = 7.3, $^3J_{HH}$ = 5.1 Hz, 1 H, Aza 5′-H), 6.12 (d, $^3J_{HH}$ = 3.7 Hz, 1 H, Aza C-3′), 6.23 (d, $^3J_{HH}$ = 2.9 Hz, 1 H, Aza 3-H), 6.52 (virtual t, J_{PH} = 7.0 Hz, 6 H, *p*-PC$_6$H$_5$),[18] 6.64 (overlapping with adjacent signal, m, 1 H, Nap 3-H), 6.77 (m, 12 H, *m*-PC$_6$H$_5$), 6.89 (d, $^3J_{HH}$ = 7.9 Hz, 1 H, Aza 4-H), 6.93 (d, $^3J_{HH}$ = 2.9 Hz, 1 H, Aza 2-H), 6.96 (d, $^3J_{HH}$ = 7.3 Hz, 1 H, Aza 4′-H), 7.23 (virtual t, J_{HH} = 7.3 Hz, 1 H, Nap 6-H), 7.37 (br., 12 H, *o*-PC$_6$H$_5$), 7.80 (d, $^3J_{HH}$ = 3.7 Hz, 1 H, Aza 2′-H), 7.91 (two overlapping signals, m, 2 H, Nap 5-H and Nap 7-

Table 4. Crystallographic parameters for complexes **4**, **5** and **7**.

	4	**5**	**7**
Colour, habit	colourless, block	yellow, lath	yellow, block
Size [mm]	0.24 × 0.14 × 0.11	0.27 × 0.07 × 0.03	0.32 × 0.26 × 0.17
Empirical formula	$C_{64}H_{55}BN_6P_2Ru$	$C_{56}H_{46.86}BCl_{0.14}N_4P_2Ru$	$C_{67}H_{57}BN_4P_2Ru$
M_r	1081.96	954.72	1091.99
Crystal system	monoclinic	monoclinic	monoclinic
Space group	$P2_1/n$	$P2_1/n$	$P2_1/c$
a [Å]	11.5818(4)	11.300(2)	21.7462(9)
b [Å]	36.4348(12)	23.663(5)	11.9883(5)
c [Å]	12.3247(4)	16.800(3)	20.7455(9)
β [°]	92.457(2)	94.275(4)	90.744(2)
V [Å^3]	5196.0(3)	4479.8(15)	5407.9(4)
Z	4	4	4
μ [mm^{-1}]	0.412	0.474	0.396
T [K]	100	100	100
$\theta_{min,max}$ [°]	2.09, 24.80	1.49, 32.81	1.94, 33.56
Completeness	0.997 to θ = 24.80°	1.000 to θ = 27.48°	1.000 to θ = 27.50°
Reflections: total/independent	100073/8943	48815/13780	205850/17693
R_{int}	0.1252	0.0534	0.0338
Final $R1$ and $wR2$	0.0506, 0.1009	0.0415, 0.0910	0.0315, 0.0851
Largest peak, hole [e Å^{-3}]	0.590, –0.959	0.821, –1.172	0.837, –0.498
$\rho_{calcd.}$ [g cm^{-3}]	1.383	1.416	1.341

H), 8.04 (two overlapping signals, m, 2 H, Nap 2-H and Nap 4-H), 8.24 (br. d, $^3J_{HH}$ = 5.1 Hz, 1 H, Aza 6′-H), 8.72 (d, $^3J_{HH}$ = 7.3 Hz, 1 H, Nap 8-H), 8.84 (br. unresolved d, 1 H, Aza 6-H) ppm. $^{13}C\{^1H\}$ NMR: δ = 102.2 and 102.4 (Aza C-3 and C-3′), 114.2 and 114.6 (Aza C-5 and C-5′), 122.7 and 122.9 (Aza C-5 and C-5′), 123.4 (Nap C-3), 124.6 (Nap 6-H), 125.4 (overlapping with solvent peaks observed by a DEPT-135 experiment, Nap C-7), 126.6, 126.7 [m, *m*-P(C_6H_5)$_3$], 128.1 (overlapping with solvent peaks observed by a DEPT-135 experiment, Nap CH), 128.4 [m, *p*-P(C_6H_5)$_3$], 128.6 (Nap C-5), 130.4 (Nap CH), 132.2 (Aza CH), 132.3 (Aza CH), 133.8 (Nap C-8), 133.9 [d, $^2J_{PC}$ = 9.9 Hz, *o*-P(C_6H_5)$_3$], 134.3 [d, $^2J_{PC}$ = 10.7 Hz, *o*-P(C_6H_5)$_3$], 136.6 [d, $^1J_{PC}$ = 38.8 Hz, *i*-P(C_6H_5)$_3$], 137.2 [d, $^1J_{PC}$ = 37.2 Hz, *i*-P(C_6H_5)$_3$], 137.8 (Aza CH), 147.9 and 150.1 (Aza C-6 and C-6′), 153.9 and 154.8 (Aza C-3a and C-3a′) ppm; a number of signals were not located or could not be assigned. $^{31}P\{^1H\}$ NMR: δ = 62.2 (d, $^2J_{PP}$ = 32.6 Hz, PPh_3), 71.3 (d, $^2J_{PP}$ = 32.6 Hz, PPh_3) ppm. $^{11}B\{^1H\}$ NMR: δ = –1.3 (v. br., $\Delta\nu_{1/2}$ = 1120 Hz) ppm. NMR spectra recorded at 22 °C: ^1H NMR (C_7D_8): δ = –14.0 (t, $^2J_{PH}$ = 26.6 Hz, 1 H, Ru-H), –2.10 (v. br., 1 H, BH, $\Delta\nu_{1/2}$ = 145 Hz), 5.88 (v. br., 2 H, Aza 5-H), 6.10 (v. br., 2 H, Aza 3-H), 6.68 (v. br., overlapping signals, 18 H, *p*-PC_6H_5, Nap 3-H and *m*-PC_6H_5), 6.94 (br., overlapping signals, 3 H, Aza 4-H and Aza 2-H), 7.20 (m, 1 H, Nap 6-H), 7.33 (br., 12 H, *o*-PC_6H_5), 7.67 (v. br., 1 H, Aza 2′-H), 7.77 (m, 1 H, Nap 7-H), 7.88 (d, $^3J_{HH}$ = 8.1 Hz, 1 H, Nap 5-H), 8.00 (d, $^3J_{HH}$ = 8.1 Hz, 1 H, Nap 4-H), 8.08 (d, $^3J_{HH}$ = 8.8 Hz, 1 H, Nap 2-H), 8.32 (v. br., 1 H, Aza 6-H), 8.57 (d, $^3J_{HH}$ = 6.7 Hz, 1 H, Nap 8-H), 8.65 (v. br., 1 H, Aza 6′-H) ppm. $^1H\{^{11}B\}$ NMR: δ = –2.10 (br., 1 H, BH, $\Delta\nu_{1/2}$ = 15 Hz) ppm. $^{13}C\{^1H\}$ NMR: δ = 102.3 (br., Aza C-3), 114.7 (br., Aza C-5), 123.2, 123.6 (Nap C-3), 124.7 (Nap C-6), 125.4 (overlapping with solvent peaks observed by a DEPT-135 experiment, Nap C-7), 126.8 [*m*-P(C_6H_5)$_3$], 126.9 (Aza C-2), 128.5 (overlapping with solvent peaks observed by a DEPT-135 experiment, Nap CH), 128.2 [*p*-P(C_6H_5)$_3$], 128.6 (Nap C-5), 130.7 (Nap CH), 132.6, 134.4 [v. br., a number of overlapping signals including *o*-P(C_6H_5)$_3$ and Nap C-8), 135.0, 138.2 [m, *i*-P(C_6H_5)$_3$], 148.6 (v. br.), 150.2 (v. br.), 154.8 (v. br.) ppm; a number of signals were not located or could not be assigned because the spectrum, particularly the azaindolyl signals, were broad at this temperature. $^{31}P\{^1H\}$ NMR: δ = 66.1 (br., PPh_3, $\Delta\nu_{1/2}$ = 79 Hz), 70.3 (br., PPh_3, $\Delta\nu_{1/2}$ = 79 Hz) ppm. $^{11}B\{^1H\}$ NMR: δ = –1.8 (s, $\Delta\nu_{1/2}$ = 210 Hz) ppm. ^{11}B NMR: δ = –1.8 (s, $\Delta\nu_{1/2}$ = 295 Hz) ppm. IR (DCM): $\tilde{\nu}$ = 2079.82 (ν_{BH}) cm^{-1}. IR (neat): $\tilde{\nu}$ = 2079 (ν_{BH}), 1899 (ν_{RuH}) cm^{-1}. $C_{60}H_{49}BN_4P_2Ru$ (999.89): calcd. C 72.07, H 4.94, N 5.60; found C 71.38, H 5.33, N 5.54. MS (ESI$^+$): m/z = 999.3 [M – H]$^+$.

Crystallography: All data were collected at 100 K with a Bruker Apex II diffractometer with an Mo-K_α radiation source (wavelength: 0.71073 Å) and an Oxford Cryosystems Cryostream low-temperature device. All data were collected by using a CCD area detector from single crystals mounted on a glass fibre. Intensities were integrated[19] from several series of exposures measuring 0.5° in ω or ϕ. Absorption corrections were made by using SADABS[20] and were based on equivalent reflections, structures were refined against all F_o^2 data. All hydrogen atoms were refined by using a riding model using SHELXL,[21] except for those attached to B, which were found in the difference map and their positions allowed to refine freely with thermal parameters limited to 1.2 times that of the boron atom. Complex **4** displayed disorder in one of the phenyl rings of the triphenylphosphane ligand. The atoms C40–C45 (phenyl) were modelled as riding over two positions. The two phenyl groups were constrained to adopt ideal six-membered ring geometry. Although, the isolated solid was spectroscopically and analytically pure, the single crystals of complex **5** contained some disordered chlorine atoms at the site of the hydrido ligand. The chlorido and hydrido ligands were refined together for the occupancy of Cl = x and the occupancy of H = 1 – x, having previously established the free refinement of the occupancy of the chlorine atom in an almost identical value (0.14 cf. 0.16). A summary of the crystallographic data collection parameters and refinement details for **4**, **5** and **7** are presented in Table 4. CCDC-839327 (for **4**), -839328 (for **5**), -839329 (for **7**) contain the supplementary crystallographic data for this paper. These data can be obtained free of charge from The Cambridge Crystallographic Data Centre via www.ccdc.cam.ac.uk/data_request/cif.

Acknowledgments

G. R. O. gratefully acknowledges the award of a Royal Society Dorothy Hodgkin Research Fellowship from the Royal Society. The

authors would like to thank the Leverhulme Trust (N. T.) for funding and Johnson Matthey for the loan of the ruthenium salts.

[1] a) D. Song, W. L. Jia, G. Wu, S. Wang, *Dalton Trans.* **2005**, 433; b) T. Saito, S. Kuwata, T. Ikariya, *Chem. Lett.* **2006**, *35*, 1224.
[2] The term "flexible scorpionate" is used to represent those ligands that contain two atoms between the boron centre and the donor atom. This additional atom provides access to a wide range of coordination modes, including those containing transition-metal–boron interactions.
[3] A. F. Hill, G. R. Owen, A. J. P. White, D. J. Williams, *Angew. Chem.* **1999**, *111*, 2920; *Angew. Chem. Int. Ed.* **1999**, *38*, 2759.
[4] a) N. Tsoureas, T. Bevis, C. P. Butts, A. Hamilton, G. R. Owen, *Organometallics* **2009**, *28*, 5222; b) N. Tsoureas, M. F. Haddow, A. Hamilton, G. R. Owen, *Chem. Commun.* **2009**, 2538; c) G. C. Rudolf, A. Hamilton, A. G. Orpen, G. R. Owen, *Chem. Commun.* **2009**, 553; d) G. R. Owen, P. H. Gould, J. P. H. Charmant, A. Hamilton, S. Saithong, *Dalton Trans.* **2010**, *39*, 392; e) G. R. Owen, P. H. Gould, A. Hamilton, N. Tsoureas, *Dalton Trans.* **2010**, *39*, 49; f) N. Tsoureas, Y.-Y. Kuo, M. F. Haddow, G. R. Owen, *Chem. Commun.* **2011**, *47*, 484.
[5] a) R. J. Blagg, C. J. Adams, J. P. H. Charmant, N. G. Connelly, M. F. Haddow, A. Hamilton, J. Knight, A. G. Orpen, B. M. Ridgway, *Dalton Trans.* **2009**, 8724; b) M. J. López-Gómez, N. G. Connelly, M. F. Haddow, A. Hamilton, A. G. Orpen, *Dalton Trans.* **2010**, *39*, 5221; c) R. J. Blagg, N. G. Connelly, M. F. Haddow, A. Hamilton, M. Lusi, A. G. Orpen, R. M. Ridgway, *Dalton Trans.* **2010**, *39*, 11616; d) M. J. López-Gómez, N. G. Connelly, M. F. Haddow, A. Hamilton, M. Lusi, U. Baisch, A. G. Orpen, *Dalton Trans.* **2011**, *40*, 4647.
[6] a) I. R. Crossley, A. F. Hill, A. C. Willis, *Dalton Trans.* **2008**, 201; b) I. R. Crossley, A. F. Hill, A. C. Willis, *Organometallics* **2008**, *27*, 312; c) I. R. Crossley, M. R. St.-J. Foreman, A. F. Hill, G. R. Owen, A. J. P. White, D. J. Williams, A. C. Willis, *Organometallics* **2008**, *27*, 381; d) I. R. Crossley, A. F. Hill, A. C. Willis, *Organometallics* **2010**, *29*, 326.
[7] a) D. J. Mihalcik, J. L. White, J. M. Tanski, L. N. Zakharov, G. P. A. Yap, C. D. Incarvito, A. L. Rheingold, D. Rabinovich, *Dalton Trans.* **2004**, 1626; b) S. Senda, Y. Ohiki, T. Hirayama, D. Toda, J.-L. Chen, T. Matsumoto, H. Kawaguchi, K. Tatsumi, *Inorg. Chem.* **2006**, *45*, 9914; c) K. Pang, S. M. Quan, G. Parkin, *Chem. Commun.* **2006**, 5015; d) K. Pang, J. M. Tanski, G. Parkin, *Chem. Commun.* **2008**, 1008; e) G. Nuss, G. Saischek, B. N. Harum, M. Volpe, K. Gatterer, F. Belaj, N. C. Moesch-Zanetti, *Inorg. Chem.* **2011**, *50*, 1991.
[8] a) S. Bontemps, M. Sircoglou, G. Bouhadir, H. Puschmann, J. A. K. Howard, P. W. Dyer, K. Miqueu, D. Bourissou, *Chem. Eur. J.* **2008**, *14*, 731; b) S. Bontemps, G. Bouhadir, W. Gu, M. Mercy, C.-H. Chen, B. M. Foxman, L. Maron, O. V. Ozerov, D. Bourissou, *Angew. Chem.* **2008**, *120*, 1503; *Angew. Chem. Int. Ed.* **2008**, *47*, 1481; c) M. Sircoglou, S. Bontemps, G. Bouhadir, N. Saffon, K. Miqueu, W. Gu, M. Mercy, C.-H. Chen, B. M. Foxman, L. Maron, O. V. Ozerov, D. Bourissou, *J. Am. Chem. Soc.* **2008**, *130*, 16729; d) M. Sircoglou, S. Bontemps, M. Mercy, K. Miqueu, S. Laderia, N. Saffon, L. Maron, G. Bouhadir, D. Bourissou, *Inorg. Chem.* **2010**, *49*, 3983; e) M.-E. Moret, J. C. Peters, *Angew. Chem. Int. Ed.* **2011**, *50*, 2063; f) C. M. Conifer, D. J. Law, G. J. Sunley, A. J. P. White, G. J. P. Britovsek, *Organometallics* **2011**, *30*, 4060.
[9] For related compounds featuring additional interactions with the transition-metal centre, see: a) J.-H. Son, M. A. Pudenz, J. D. Hoefelmeyer, *Dalton Trans.* **2010**, *39*, 11081; b) X. Zhao, E. Otten, D. Song, D. W. Stephan, *Chem. Eur. J.* **2010**, *16*, 2040; c) D. J. H. Emslie, L. E. Harrington, H. A. Jenkins, C. M. Robertson, J. F. Britten, *Organometallics* **2008**, *27*, 5317.
[10] a) H. Braunschweig, R. D. Dewhurst, *Dalton Trans.* **2011**, *40*, 549; b) A. Amgoune, D. Bourissou, *Chem. Commun.* **2011**, *47*, 859; c) G. Bouhadir, A. Amgoune, D. Bourissou, *Adv. Organomet. Chem.* **2010**, *58*, 1; d) G. R. Owen, *Transition Met. Chem.* **2010**, *35*, 221; e) J. I. van der Vulgt, *Angew. Chem. Int. Ed.* **2010**, *49*, 252; f) H. Braunschweig, R. D. Dewhurst, A. Schneider, *Chem. Rev.* **2010**, *110*, 3924; g) K. I. Kuzu, I. Krummenacher, F. Armbruster, F. Breher, *Dalton Trans.* **2008**, 5836; h) F.-G. Fontaine, J. Boudreau, M.-H. Thibault, *Eur. J. Inorg. Chem.* **2008**, 5439; i) A. F. Hill, *Organometallics* **2006**, *25*, 4743; j) G. Parkin, *Organometallics* **2006**, *25*, 4744; k) H. Braunschweig, C. Kollann, D. Rais, *Angew. Chem.* **2006**, *118*, 5380; *Angew. Chem. Int. Ed.* **2006**, *45*, 5254.
[11] a) G. R. Owen, N. Tsoureas, A. Hamilton, A. G. Orpen, *Dalton Trans.* **2008**, 6039; b) G. Dyson, A. Hamilton, B. Mitchell, G. R. Owen, *Dalton Trans.* **2009**, 6120; c) N. Tsoureas, J. Nunn, T. Bevis, M. F. Haddow, A. Hamilton, G. R. Owen, *Dalton Trans.* **2011**, *40*, 951; d) G. R. Owen, N. Tsoureas, R. F. Hope, Y.-Y. Kuo, M. F. Haddow, *Dalton Trans.* **2011**, *40*, 5906.
[12] a) S. Trofimenko, *J. Am. Chem. Soc.* **1966**, *88*, 1842; b) S. Trofimenko in *Scorpionates: The Coordination of Poly(pyrazolyl) borate Ligands*, Imperial College Press, London, **1999**; c) S. Trofimenko, *Chem. Rev.* **1993**, *93*, 943; d) S. Trofimenko, *Polyhedron* **2004**, *23*, 197; e) C. Pettinari in *Scorpionates II: Chelating Borate Ligands*, Imperial College Press, London, **2008**.
[13] a) M. Jiménez-Tenorio, M. C. Puerta, P. Valerga, *Inorg. Chem.* **1994**, *33*, 3515; b) P. S. Hallman, D. Evans, J. A. Osborn, G. Wilkinson, *Chem. Commun. (London)* **1967**, 305.
[14] R. J. Abernethy, A. F. Hill, N. Tshabang, A. C. Willis, R. D. Young, *Organometallics* **2009**, *28*, 488.
[15] M. Jiménez-Tenorio, M. C. Puerta, P. Valerga, *Organometallics* **2009**, *28*, 2787.
[16] One of these signals overlapped with the PC_6H_5 signals. Its location was confirmed by a correlation experiment.
[17] I. R. Crossely, A. F. Hill, A. C. Willis, *Organometallics* **2006**, *25*, 289.
[18] W. H. Hersh, *J. Chem. Educ.* **1997**, *74*, 1485.
[19] *SAINT*, V7.53A, Bruker-AXS, Madison, WI, **2008**.
[20] G. M. Sheldrick, *SADABS*, V2008/1, University of Göttingen, Göttingen, **2008**.
[21] G. M. Sheldrick, *Acta Crystallogr., Sect. A* **2008**, *64*, 112.

Received: August 16, 2011
Published Online: October 28, 2011

